Acta Mech. Sin. (2015) 31(5):685–697
DOI 10.1007/s10409-015-0466-x

RESEARCH PAPER

On the degradation of granular materials due to internal erosion

Xiaoliang Wang[1] · **Jiachun Li**[1]

Received: 30 January 2015 / Revised: 22 April 2015 / Accepted: 4 May 2015 / Published online: 14 July 2015

Abstract A new state-based elasto-plastic constitutive relationship along with the discrete element model is established to estimate the degradation of granular materials due to internal erosion. Four essential effects of internal erosion such as the force network damage and relaxation are proposed and then incorporated into the constitutive relationship to formulate internal erosion impacts on the mechanical behavior of granular materials. Most manifestations in the degradation of granular materials, such as reduction of peak strength and dilatancy are predicted by the modified constitutive relationship in good agreement with the discrete element method (DEM) simulation. In particular, the sudden reduction of stress for conspicuous mass erosion in a high stress state is captured by force network damage and the relaxation mechanism. It is concluded that the new modified constitutive relationship is a potential theory to describe the degradation of granular materials due to internal erosion and would be very useful, for instance, in the prediction and assessment of piping disaster risk during the flood season.

Keywords Internal erosion · Degradation · Granular materials · Discrete element method

✉ Jiachun Li
jcli05@imech.ac.cn

Xiaoliang Wang
wangxiaoliang@imech.ac.cn

[1] Key Laboratory for Mechanics in Fluid Solid Coupling Systems, Institute of Mechanics, Chinese Academy of Sciences, No. 15 Beisihuanxi Road, Beijing 100190, China

1 Introduction

During flooding at the high water stage, fine particles in a dam or levee are very likely eroded and then washed away by hydraulic force and seepage flow. This phenomena is called internal erosion, which takes place frequently in water conservancy systems, and may cause catastrophic disaster and claim a large number of human lives. For instance, the flood of Heilongjiang in the summer of 2013 broke a couple of fissures in levees through internal erosion. Internal erosion-induced hazards happen time and again over the world as well [1].

Internal erosion, including piping and suffusion, usually experiences three mutually coupled processes, namely seepage, particle initiation/transport, and structure response [2]. As the high hydraulic gradient initiates and carries away fine particles, the particle removal further enlarges porosity and thus results in stronger seepage flow. Similarly, the reduction of effective stress due to high pore pressure tends to increase fluidity and permeability again. The degradation of soil structure becomes a hidden risk for the safety of the levee's structure. However, this is often ignored in geotechnical engineering design for soil structures.

Most experimental and numerical studies are devoted to the issue of the coupling of seepage flow and particle transport [3–7], which mainly includes an initiation criterion, transport rate, and influences on the granular material structures. In the monograph *Erosion of Geomaterials* [8], almost all the chapters deal with the initiation criterion and transport properties. On the one hand, we need to notice the softening of saturated granular materials due to the physicochemical roles of water in porous media [9]. On the other hand, we find that the issue concerning how the variation in stress affects initiation and transport of particles

is seldom paid attention to. In particular, the degradation of granular materials and the response of soil structure due to internal erosion could only be found in very few papers.

A three-phase continuum mechanical model for the fluidization and erosive process was established by Vardoulakis [2]; however, the degradation of granular material due to erosion is ignored. In their study, Papamichos et al. [10,11] made several sand production experiments in a hollow cylinder with a cavity. Later, they simulated the sand production process with a new hydro-mechanical model. With regard to constitutive law, the effect of internal erosion is considered a stress variation corresponding to porosity growth, which is very similar to Hicher's method [12]. Unfortunately, crude treatment, only convenient for finite element analysis, was unable to reveal fully the degradation mechanism in internal erosion. The paper by Sterpi et al. [13] analyzed the settlement due to erosion and transport of fine particles induced by groundwater pumping from a drainage trench by their hydro-mechanical model, in which the degradation of material behavior is attributed to the variation of relative density. In the three-fields coupling model of Nishimura et al. [14], only the variation in critical state due to particle removal is considered in his constitutive law. The study by Scholtès et al. [15] used the discrete element method (DEM) to examine the degradation of granular materials due to particle removal. A micromechanical model was invented by Hicher [12] to simulate the effects of particle removal on the mechanical behavior of granular materials. The work fails to predict the stress reduction because it only accounts for volume contraction, which happens when the eroded granular assembly cannot recover to its original stress state. In addition, the micromechanical formulation is so complicated that it is hard to be implemented in finite element analysis.

Up to now, implied physical mechanisms for the degradation of granular materials by internal erosion remain unrevealed. Furthermore, the model should be formulated in a unified framework to facilitate theoretical analysis and finite element simulation. The foregoing two objectives motivate us to establish a new state-based elasto-plastic constitutive relationship along with discrete element model to describe the degradation of granular materials due to internal erosion.

2 State-based elasto-plastic relationship for granular materials

Mechanical behavior of granular material heavily depends on the granular arrangement states, which generally is ignored in the conventional constitutive relationship of Cam-clay. Research by Manzari and Dafalias [16] proposed an elasto-plastic model with two yield surfaces for sand, in which the dilatancy for triaxial extension and compression are different. Based on their former concept of sand state, Cubrinovski and Ishihara [17] developed a stress-strain-dilatancy relationship where the dilatancy depends on the equivalent plastic strain in the following year. Then, Gajo and Wood [18] presented a constitutive law for sand based on critical state, called Severn-Trent by them, which could reflect the influences of internal state on the dilatancy of sand. Housbly [19] proposed the famous hyperplasticity theory based on the internal variable theory developed from non-equilibrium thermodynamics. In 1998, Wan and Guo [20] introduced void ratio into the dilatancy equation to establish a constitutive law for sand based on current state. In the new century, Li and Dafalias [21] proposed a theory for state-dependent dilatancy for the first time in the geotechnical community. Namely, the dilatancy is a function of stress ratio, void ratio, and other internal state variables in this new relationship. In order to couple with the erosion process more efficiently, a simple state-dependent elasto-plastic relationship given by Wood [22] is used in this study. However, any of the above state-based constitutive laws could be regarded as a framework to consider the internal erosion.

2.1 Internal state description

There are several kinds of expressions to represent the current state of sand. The equation proposed by Been and Jefferies [23] is chosen, where the so-called current state means the differences between current specific volume and critical specific volume under the same effective stress as shown in Eq. (1)

$$\psi = v - v_c, \tag{1}$$

where ψ represents the current state of sand, v and v_c are the current specific volume and critical specific volume, respectively. Evidently, $\psi > 0$ means sand is in a loose state, $\psi = 0$ means in the critical state, and $\psi < 0$ means in a dense state.

The critical state of granular material obeys Eq. (2)

$$v = \Gamma - \lambda \left(\frac{p'}{p_a}\right)^{\xi}, \tag{2}$$

where v is the specific volume, p' is the mean effective normal stress, p_a is the atmospheric pressure, and Γ, λ and ξ are material parameters, which can be obtained by fitting Eq. (2) with the isotropic consolidation tests or 1-D compression test.

2.2 Yield criterion, flow rule, and hardening rule

The Mohr–Coulomb criterion is used as a yield function for granular materials, as shown in Eq. (3)

$$f = q - \eta_y p', \tag{3}$$

in which q is the deviatoric stress, η_y is the hardening variable controlling the size of current yield surface.

The non-associate flow rule is used to describe the flow of plastic strain. Critical state should also be considered and incorporated into the constitutive law; the plastic potential function can be shown in Eq. (4)

$$g = q - Mp' \ln \frac{p_{\mathrm{r}}}{p'}, \tag{4}$$

where M is the stress ratio at the critical state and p_{r} is a reference pressure.

The hardening rule is expressed as a hyperbolic function of shear plastic strain in Eq. (5)

$$\frac{\eta_y}{\eta_p} = \frac{\varepsilon_q^p}{a + \varepsilon_q^p}, \tag{5}$$

where η_y is the current peak stress ratio, $\varepsilon_q^{\mathrm{p}}$ is the plastic shear strain, and a is a physical parameter. η_p represents the potential strength in the current state, which depends on the current state of granular materials. Here, a linear function between η_p and the current state of granular materials is assumed in Eq. (6)

$$\eta_p = M - k\psi. \tag{6}$$

2.3 Constitutive law

The elastic response is expressed in Eq. (7)

$$\begin{pmatrix} \mathrm{d}p \\ \mathrm{d}q \end{pmatrix} = \begin{bmatrix} K & 0 \\ 0 & 3G \end{bmatrix} \begin{pmatrix} \mathrm{d}\varepsilon_p \\ \mathrm{d}\varepsilon_q \end{pmatrix} = \boldsymbol{D}_{\mathrm{e}} \begin{pmatrix} \mathrm{d}\varepsilon_p \\ \mathrm{d}\varepsilon_q \end{pmatrix}, \tag{7}$$

where K is the bulk modulus, G is the shear modulus, and $\boldsymbol{D}_{\mathrm{e}}$ is the elastic stiffness matrix. The following isotropic stress-dependent elastic relations are employed [24]

$$G = G_0 \frac{(2.97 - e)^2}{1 + e} \sqrt{pp_{\mathrm{a}}}, \quad K = G \frac{2(1 + \nu_p)}{3(1 - 2\nu_p)}, \tag{8}$$

in which e is void ratio, ν_p is Poisson's ratio, and G_0 is material parameter.

The above constitutive law is a state-dependent constitutive law, and one can find that the dilatancy equation is dependent on both stress ratio and current state.

By standard mathematical manipulation of elasto-plastic theory, we can derive a stress-strain equation like Eq. (9)

$$\begin{pmatrix} \mathrm{d}p \\ \mathrm{d}q \end{pmatrix} = \boldsymbol{D}_{\mathrm{e}p} \begin{pmatrix} \mathrm{d}\varepsilon_p \\ \mathrm{d}\varepsilon_q \end{pmatrix}, \tag{9}$$

where $\boldsymbol{D}_{\mathrm{e}p} = \boldsymbol{D}_{\mathrm{e}} - \frac{\boldsymbol{D}_{\mathrm{e}} \frac{\partial g}{\partial \sigma} \frac{\partial f}{\partial \sigma}^{\mathrm{T}} \boldsymbol{D}_{\mathrm{e}}}{\frac{\partial f}{\partial \sigma}^{\mathrm{T}} \boldsymbol{D}_{\mathrm{e}} \frac{\partial g}{\partial \sigma} + H} \alpha$ and $\alpha = \begin{cases} 1, & \textit{Loading} \\ 0, & \textit{Unloading} \end{cases}$,

in which H given by Eq. (10) is the hardening function depending on both the stress ratio and the state variation

$$\begin{aligned} H &= -\frac{\partial f}{\partial \kappa} \frac{\partial \kappa^{\mathrm{T}}}{\partial \varepsilon_{ij}^p} \frac{\partial g}{\partial \sigma_{ij}} \\ &= p' \left[(M - \eta_y) \frac{\eta_y}{\eta_p} k v_0 + \frac{(\eta_p - \eta_y)^2}{a \eta_p} \right]. \end{aligned} \tag{10}$$

As a result, the constitutive law Eq. (9) along with the hardening law Eq. (10) is capable of modeling the state-dependent behavior of granular materials for different initial porosities [22].

3 Four essential effects of internal erosion

If some particles are removed at certain stress states of granular materials, internal structures then change immediately. The particle removal has at least two macroscopic effects on the mechanical behavior as observed in both experiment and DEM simulation. An apparatus designed by Chang and Zhang [4] models the piping process under a specified stress state. In their experiment, both dilatancy and peak friction strength are decreasing during internal erosion. Similarly, DEM simulation [25,26] showed the same tendency when considering the impact of particle removal on mechanical behavior. Therefore, we may conclude that internal erosion considerably degrades the mechanical behavior of granular materials. In this section, the internal erosion is decomposed into four essential effects on the degradation of granular material.

3.1 The "Loose" effect

As soon as particle removal occurs, the current void ratio instantly increases, thus leading to an unstable granular structure. The void ratio after particle removal becomes

$$e' = \frac{e + D}{1 - D}, \tag{11}$$

where indicator D represents mass erosion percentage, defined as the ratio of eroded mass and the total mass in a representative volume element. Evidently, $e' > e$ implies

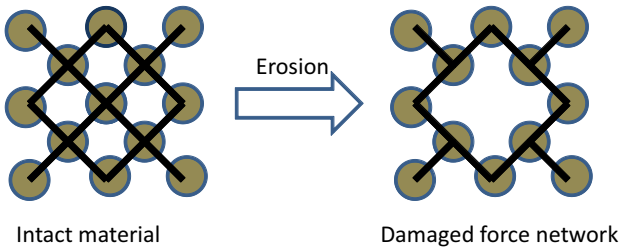

Fig. 1 Illustration of force network damage of granular materials. The *brown circles* represent particles, and the *solid black line* represents contact force between contacting particles

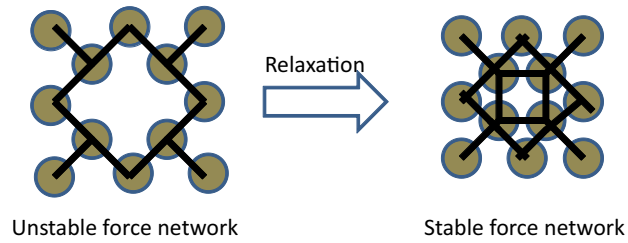

Fig. 2 Illustration of force network relaxation of granular materials. The *brown circles* represent particles, and the *solid black line* represents contact force between contacting particles

that the void ratio usually is increasing during particle erosion.

3.2 Force network damage

After removal of some particles, the interactions between them disappear and the force chains involved with those particles are suddenly broken as shown in Fig. 1. This effect of internal erosion is called force network damage (FND). Moreover, this phenomenon can be simulated in DEM, but is very difficult to be observed in experiments owing to swift loading speed and instantaneous particle rearrangement. Breakage of several force chains leads to a damage in the macroscopic force network and a few local FNDs results in stress reduction. Namely, the damage is manifested in two forms: the reduction of hydrostatic stress and deviatoric stress as seen in Eq. (12).

$$\begin{aligned} \delta\, p_d &= f_{pd}(p, q, D), \\ \delta\, q_d &= f_{qd}(p, q, D), \end{aligned} \tag{12}$$

in which δp_d and $\delta\, q_d$ are hydrostatic stress reduction and deviatoric stress reduction in the FND, respectively. The FND function f_{pd} and f_{qd} are assumed to depend on the stress states and mass erosion percentage for a specified particle size distribution. p, q, and D denote hydrostatic stress, deviatoric stress and mass erosion percentage, respectively.

3.3 Force network relaxation

With force network damage, the force network usually is no longer in an equilibrium state. The unstable granular system will relax to a stable state by itself, as shown in Fig. 2, which is called force network relaxation (FNR). If the eroded mass is small, there is no volume contraction in the relaxation. However, if the eroded mass is conspicuous, a volume contraction inevitably happens in the relaxation process. The evolution law of FNR can be represented in Eq. (13).

$$\begin{aligned} \delta\, p_r &= f_{pr}(p, q, D), \\ \delta\, q_r &= f_{qr}(p, q, D), \\ \delta\varepsilon_V &= f_{\varepsilon r}(p, q, D). \end{aligned} \tag{13}$$

Similar to the assumption made in FND, the relaxation law is assumed to depend on the stress states and erosion mass for a specific granular assembly with a certain particle size distribution. δp_r, $\delta\, q_r$, and $\delta\varepsilon_V$ denote the hydrostatic stress reduction, deviatoric stress reduction, and volume contraction in the relaxation process.

In the model of Hicher [12] and Papamichos [10], all the effects of internal erosion are regarded as the "loose" effect in Sect. 3.2, and a volume contraction, which occurs when the eroded granular material can recover to the original stress state by external loading. However, the instant stress reduction cannot be modeled when a conspicuous mass erosion event occurs at a high stress state in their models. In contrast, the separation of internal erosion effects into FND and FNR can handle this issue, as can be seen in the later passage.

3.4 Variation of critical state

The critical state of granular materials depends on particle size distribution, as shown by Wood [27] in modeling the effects of particle crush on mechanical behavior of granular materials. Both internal erosion and particle crush change the particle size distribution: the former reduces the fine grains content, while the latter increases the fine grain contents. In Wood's equation, the variation of particle size distribution is modeled as the fractal coefficient deviation from the natural particle size distribution of sands.

Nevertheless, the eroded mass percentage D is chosen as the state variable. Then the critical state line becomes a series of lines with D as a parameter. As a simplification, only the coefficient is assumed as a function of D in Eq. (2), as shown in Eq. (14)

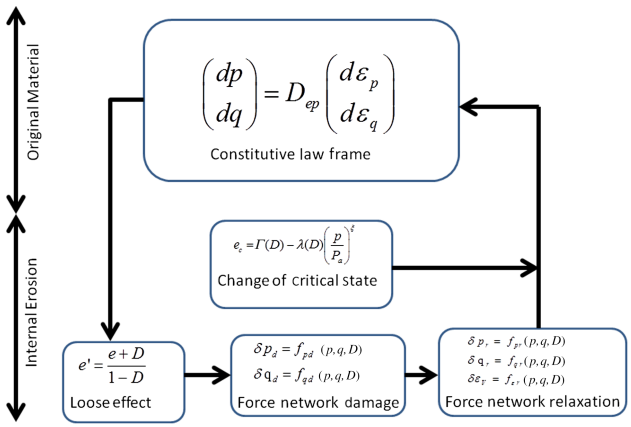

Fig. 3 Mathematical model of the degradation of granular materials due to internal erosion

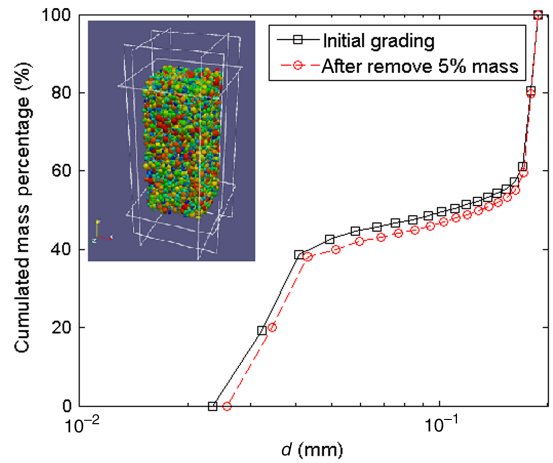

Fig. 4 Numerical triaxial apparatus and particle size distribution for the virtual granular material

$$\nu = \Gamma(D) - \lambda(D)\left(\frac{p}{P_a}\right)^{\xi}. \tag{14}$$

3.5 Unified framework for degradation due to internal erosion

Combining the mathematical models of the four effects, the degradation due to internal erosion on mechanical behavior can be unified into a constitutive relationship. If one erosion event happens, a "loose" effect takes place, then FND and FNR play roles, during which the critical state changes correspondingly. The simulation is performed by following this order, as illustrated in Fig. 3.

4 Determination of internal erosion effects

In order to understand better the mechanical processes that happen during the internal erosion, a DEM model is established to simulate these processes. Several DEM simulations are implemented to determine the internal erosion effects.

4.1 Discrete element model

The DEM has made great progress in both fundamental and field research in soil and rock mechanics since its proposal by Cundall in 1979 [28]. Up to now, several open source platforms based on DEM are available, among which Yade [29] is used in this study because of its flexibility.

A numerical triaxial apparatus [25,26] is designed to investigate the impact of particle removal on the mechanical behavior of granular materials. Firstly, an assembly of particles is isotropically consolidated to a specified pressure, and then a triaxal load is applied to achieve a stress state. When some particles are removed, the triaxial load is applied again until the sample fails. A series of Python subroutines are designed to remove the particles together with the interactions involved. Both the eroded mass percentage and the stress state during the process can be specified by users. In addition, some subroutines are designed to extract different contributions of contact force chains, such as the stress due to eroded particles, strong/weak contribution forces.

In DEM, interactions between particles are decomposed into a normal part F_n and a shear part F_s; the normal stiffness and shear stiffness are defined by contact modulus Y and stiffness ratio α equivalently, as shown in Eqs. (15) and (16)

$$k_n = 2 \times \frac{Y \times R_1 \times R_2}{(R_1 + R_2)}, \tag{15}$$

$$k_s = \alpha \times k_n, \tag{16}$$

where R_1 and R_2 are radii of the two contacting particles.

The tangential force obeys the Coulomb friction law like Eq. (17)

$$F_s \leqslant \mu F_n = \tan\Phi F_n, \tag{17}$$

in which μ is friction coefficient, Φ, is the interparticle friction angle.

Since the mechanism and constitutive modeling are the main objects, only a virtual granular material with particle size distribution shown in Fig. 4 is generated. As for real granular material, the rolling resistance contact model should be used to account for the non-spherical particle effect. Contact parameters must also be calibrated against typical triaxial experiments [30].

In piping disaster, if hydraulic gradient reaches a critical value, fine particles could be eroded away by hydraulic

force and seepage flow, leaving coarse grains to support external loads. It is feasible to realize this kind of virtual test in numerical triaxial apparatus although we can hardly remove certain percentage of particle mass in a physical triaxial compression experiment. In DEM, we remove fine particles of a specified mass percentage at a specified stress ratio, while cancelling the interaction associated with them to simulate the initiation and transport of fine particles during internal erosion.

In the numerical cell, 40000 particles were generated. The basic illustration of the numerical triaxial apparatus and the particle size distribution for the virtual granular material is shown in Fig. 4. As a matter of fact, this kind of psd represents poor grade soil, in which both coarse and fine particles dominate in order to facilitate examining the following cases: coarse grains form skeleton, while fine grains can be easily flooded away by seepage flow. All of the parameters relevant to contact information in DEM simulation are specified as: $Y = 100$ MPa, stiffness ratio $\alpha = 0.4$, and particle friction angle $\Phi = 30°$. The confining stresses are 50 kPa in all the simulation and theoretical analysis. The corresponding bulk modulus, Poisson's ratio, peak and residual friction angle for the virtual granular material are 16.2 MPa, 0.35, 35°, and 19°, respectively.

The above numerical triaxial apparatus can be used to examine the triaxial compression with and without particle removal in this study.

In order to examine the internal erosion effects, a subtle change of the numerical triaxial apparatus is implemented to determine the actual form of FND and FNR for the virtual granular material. When erosion starts, the sample boundary is kept fixed to exclude the influence of external loading. The force network involved in the removed particle is calculated. Then the sample is free to relax to a stable state. If the eroded mass percentage is conspicuous, the force network may be unable to support the volume prior to particle removal, so the vertical plate of the triaxial apparatus is moved inwards if the mean stress is less than a small stress, and thus there will be a volume contraction in this case.

4.2 Law of FND

In the erosion test, stress ratio and mass erosion percentage are two major factors. Here, eight parameters for mass erosion percentage and four for the stress ratio, together 32 cases, are simulated to test the force network damage and force network relaxation processes. Force reduction of hydrostatic stress and deviatoric stress in FND are shown in Fig. 5 in dimensionless form. The hydrostatic stress reduction as a function of the mass erosion percentage D is independent of stress ratio. The deviatoric stress reduction is proportional to the stress ratio and passing through the origin. If putting the FND law into dimensionless form, only two dimensionless variables are involved in the FND law, which obeys linear relationship.

The coefficient of FND is a function of D, which is numerically fitted by using a linear function, as shown in Fig. 6. The FND law is finally derived like Eq. (18).

$$\begin{aligned} \frac{\delta p_d}{p} &= -3.48D, \\ \frac{\delta q_d}{p} &= -2.62D\frac{q}{p}. \end{aligned} \tag{18}$$

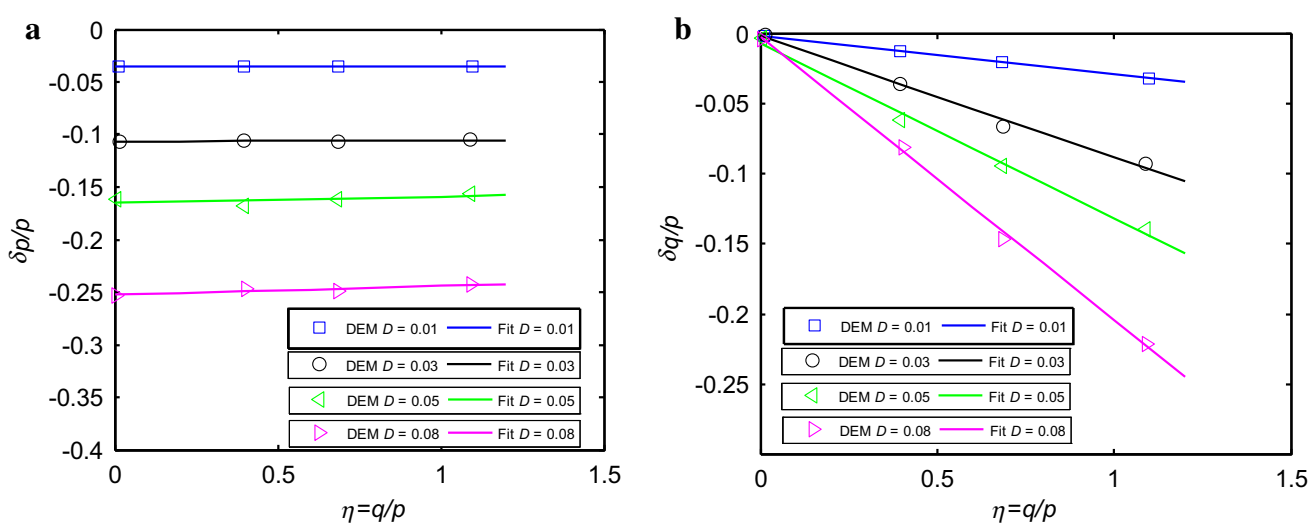

Fig. 5 Stress reduction in force network damage. **a** Hydrostatic stress reduction. **b** Deviatoric stress reduction

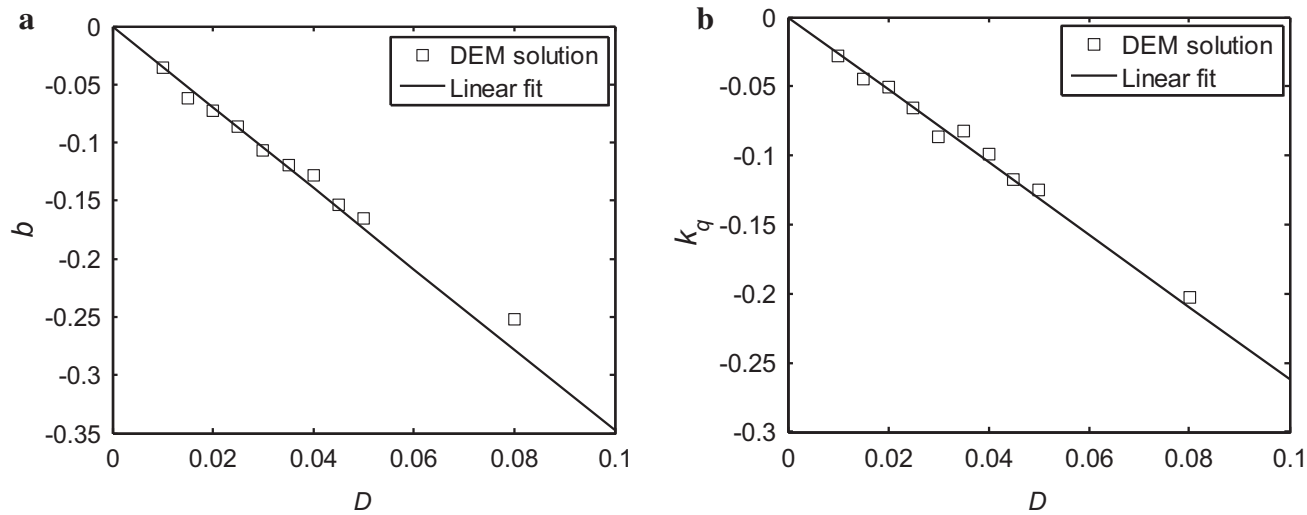

Fig. 6 Linear fit for the coefficient of FND law. **a** Hydrostatic stress reduction. **b** Deviatoric stress reduction

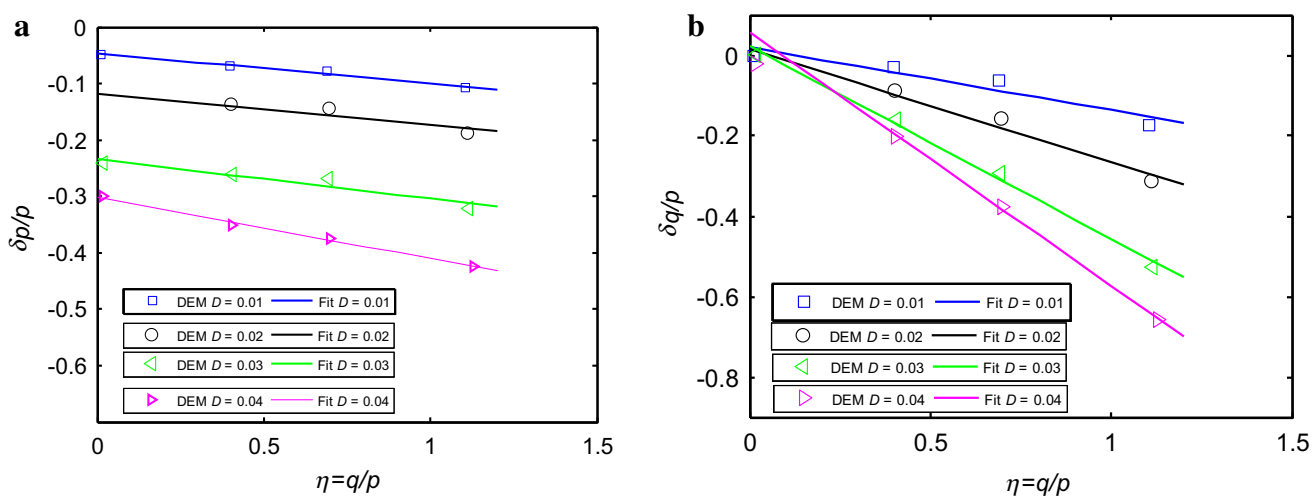

Fig. 7 Stress reduction in force network relaxation. **a** Hydrostatic stress reduction. **b** Deviatoric stress reduction

4.3 Law of FNR

When particle removal occurs, the new force network is no longer in equilibrium state. As a result, some particles tend to find new contacts with their neighboring particles, others to adjust their contact force. Then, while the old force network breaks, a new force network in equilibrium forms. The evolution of the unstable system to a stable system is similar to a kind of relaxation process which is called force network relaxation. The reduction of hydrostatic stress and deviatoric stress in FNR process is shown in Fig. 7, from which it is found that the linear relationship still holds for FDR. The fits for the coefficient of hydrostatic stress relaxation and deviatoric stress relaxation are shown in Fig. 8. The fitting result is better for small mass erosion than that for conspicuous mass erosion. The final law of FNR is obtained in Eq. (19).

$$\begin{aligned} \frac{\delta p_{\mathrm{r}}}{p} &= -0.41\sqrt{D}\frac{q}{p} - 0.87D, \\ \frac{\delta q_{\mathrm{r}}}{p} &= -15.89D\frac{q}{p} \end{aligned} \tag{19}$$

As indicated in FND and FNR tests, if conspicuous mass erosion happens at high stress state, the eroded granular assembly is so weak that not only a relaxation of both hydrostatic and deviatoric stresses exist, but also a volume contraction phenomenon is observed in this case as shown in Fig. 9. Based on these tests we find that there is no volume contraction in the relaxation for mass erosion percentage less than 4 %, while a volume contraction takes place for mass erosion percentage larger than 4 % for the virtual granular material. In addition, the volume contraction is only dependent on the mass erosion percentage and independent of the stress state. An exponential function is used to fit the volume contrac-

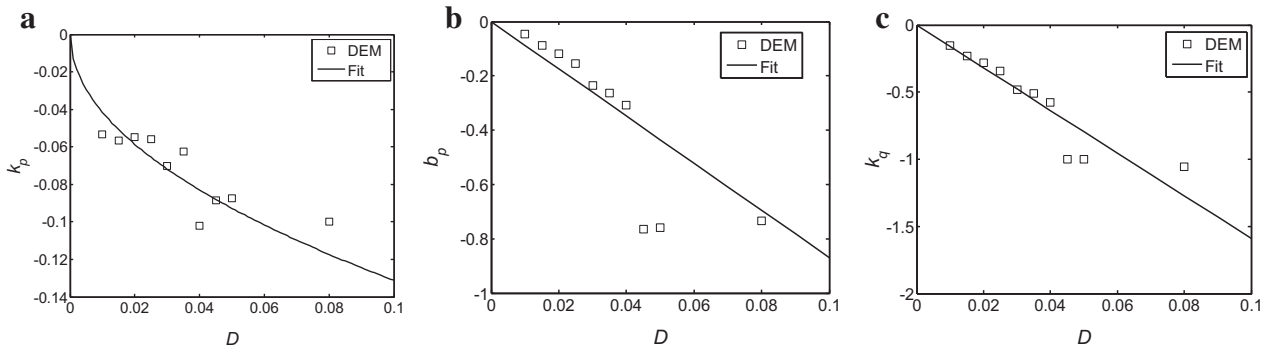

Fig. 8 Curve fit for the coefficients in the linear law of FNR. **a** Fit for the slope of hydrostatic stress reduction in FNR. **b** Fit for the intersection of hydrostatic stress reduction in FNR. **c** Fit for deviatoric stress reduction in FNR

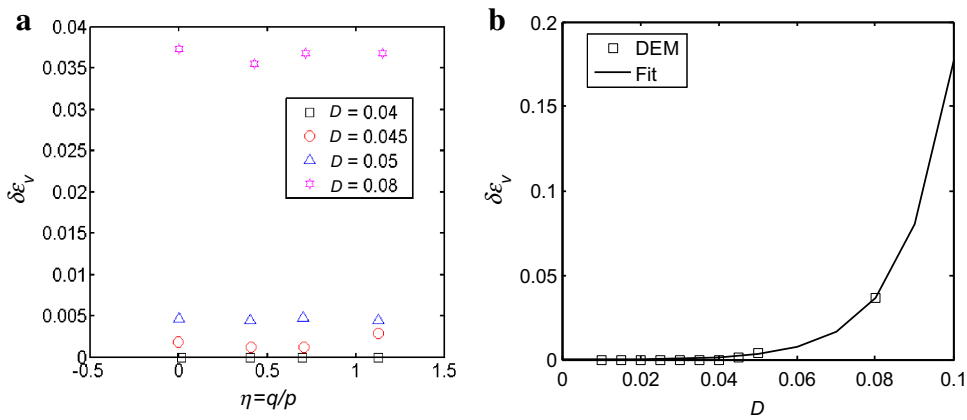

Fig. 9 Volume contraction during force network relaxation process and the fit. **a** Volume contraction. **b** Fit for the volume contraction law

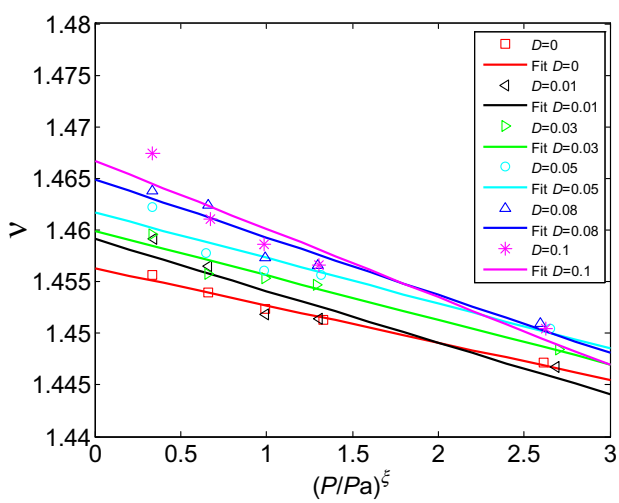

Fig. 10 Critical state lines corresponding to different erosion mass percentages with their fits

tion, as shown in Fig. 9. The volume contraction law is then derived in exponential form, which can been seen in Eq. (20).

$$\delta\varepsilon_V = 0.0001\exp(79\,D). \tag{20}$$

4.4 Variation of critical state

As for the virtual granular material simulation for each eroded mass percentage case, a series of triaxial compression tests with confining pressure 25, 50, 75, 100, and 200 kPa are performed. By extracting the data of critical states, five points for each erosion case are obtained. Figure 10 plots the fitting results of Eq. (14) for each case. The fitting result shows that internal erosion causes the critical state line to move upward in the $\nu - P$ plane, and the final expression is shown in Eq. (21). The 3-D surface of the critical state is shown in Fig. 11.

$$\begin{aligned} \Gamma(D) &= 0.0965\,D + 0.4571, \\ \lambda(D) &= 0.0232D + 0.0039. \end{aligned} \tag{21}$$

5 Model validation and prediction

5.1 Model parameters

If incorporating the "loose" effect, FND, FNR, and the variation of critical state into the original state-dependent

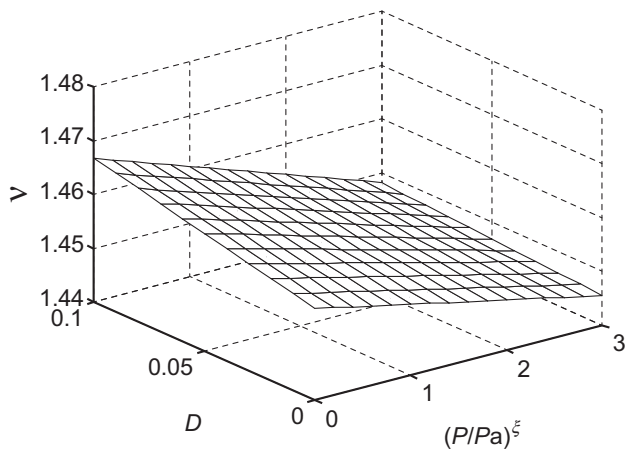

Fig. 11 3D surface of the critical state of granular materials considering internal erosion

Table 1 Values of the parameters in the constitutive law

Elastic parameters	Critical state parameters	Parameters of plasticity
$G_0 = 46.8$	$M = 0.73$	$k = 11.0$
$v_p = 0.35$	$\Gamma = 1.459$	$a = 0.001$
	$\lambda = 0.006$	
	$\xi = 1.0$	

constitutive law, the degradation of granular materials due to internal erosion is formulated in a unified framework of the constitutive law as shown in Fig. 6. The physical laws of the four effects for the virtual granular material with a certain particle size distribution shown in Fig. 1 are deduced in part 3 and part 4. The remaining issue for this constitutive law is how to determine those constitutive parameters including two for elasticity, two for plasticity and the remaining four for critical state, together with the initial conditions. The parameters of elasticity, critical state, and initial conditions are readily derived in the triaxial compression tests for the granular assembly under no internal erosion. The two parameters in the hardening law of plasticity, a and k, are obtained via calibration in the triaxial compression tests under no particle removal. All the parameters obtained are shown in Table 1. The constitutive law is now capable of predicting all cases with or without particle removal in the triaxial compression test.

The response of the triaxial compression test with no particle removal is directly predicted by the constitutive relationship as shown in Fig. 12. We find that this result coincides well with the DEM simulation including hardening and softening processes. In addition, the dilatancy is also well captured. Hence, the constitutive law we proposed is validated to be able to model the main mechanical feature of granular material quantitatively.

5.2 Response prediction for different mass erosion percentages

By incorporation of the four effects, the constitutive law is used to predict the degradation of granular material due to particle removal. In the DEM simulation counterpart, triaxial loading is stopped when consolidation ends, particles of different mass percentages of 1 %, 3 %, and 5 % are removed and then triaxial loading is applied again until the granular assembly fails. The prediction of this internal erosion process in triaxial compression tests is implemented by the constitutive relationship with results shown in Fig. 13. The main

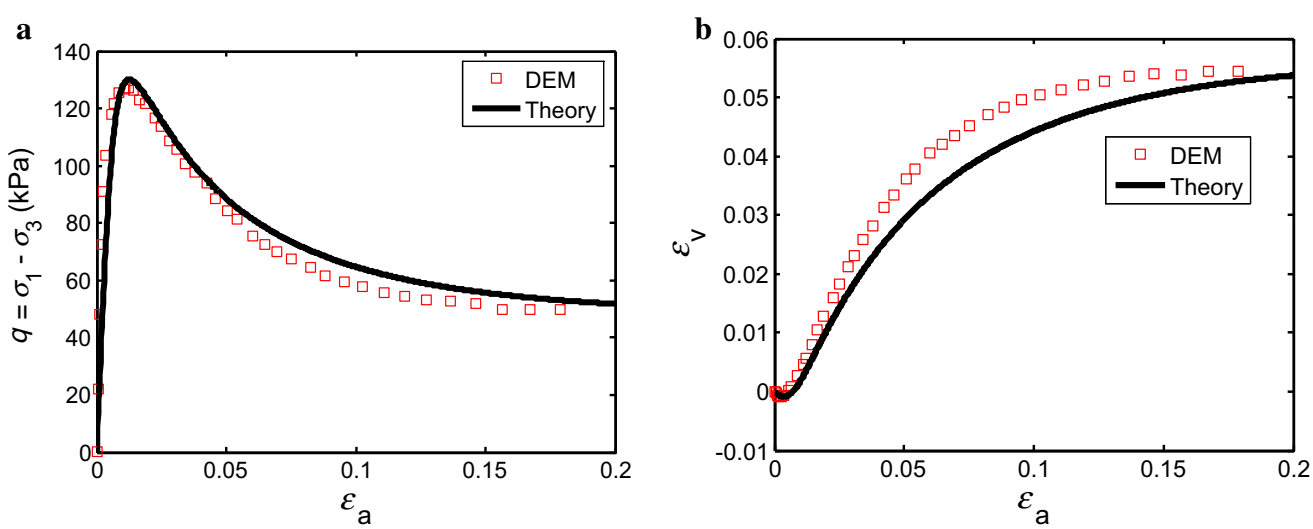

Fig. 12 Prediction of the triaxial compression tests via the constitutive law and its comparison with the DEM simulation. **a** Stress-strain response. **b** Volume-axial strain response

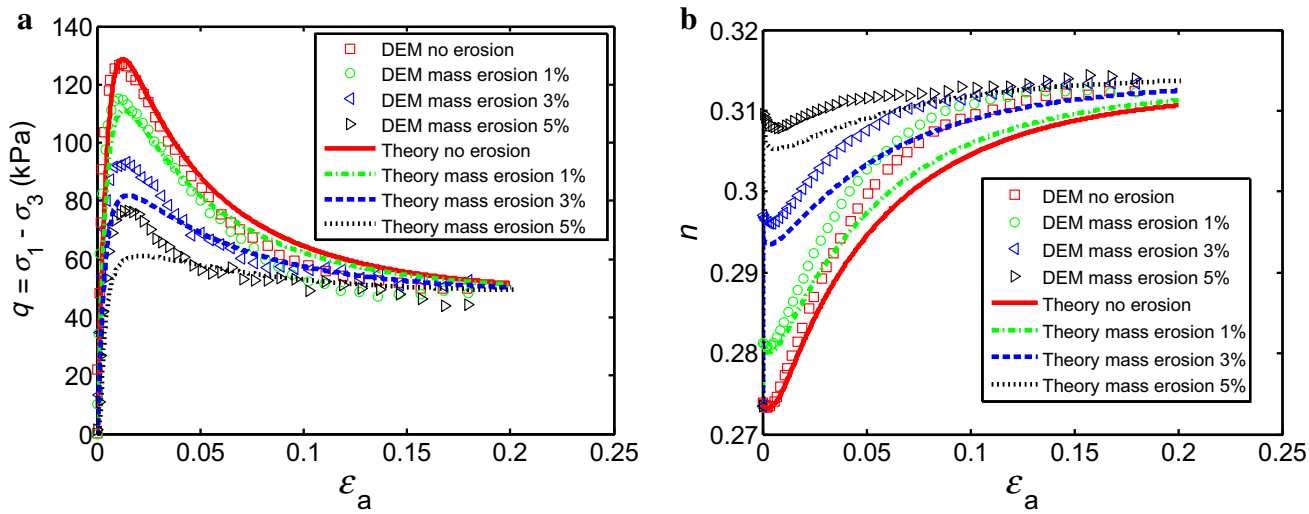

Fig. 13 Prediction of the mechanical behavior of granular material under internal erosion in a triaxial compression test by both constitutive relationship and DEM simulation. **a** Stress-strain response. **b** Porosity evolution

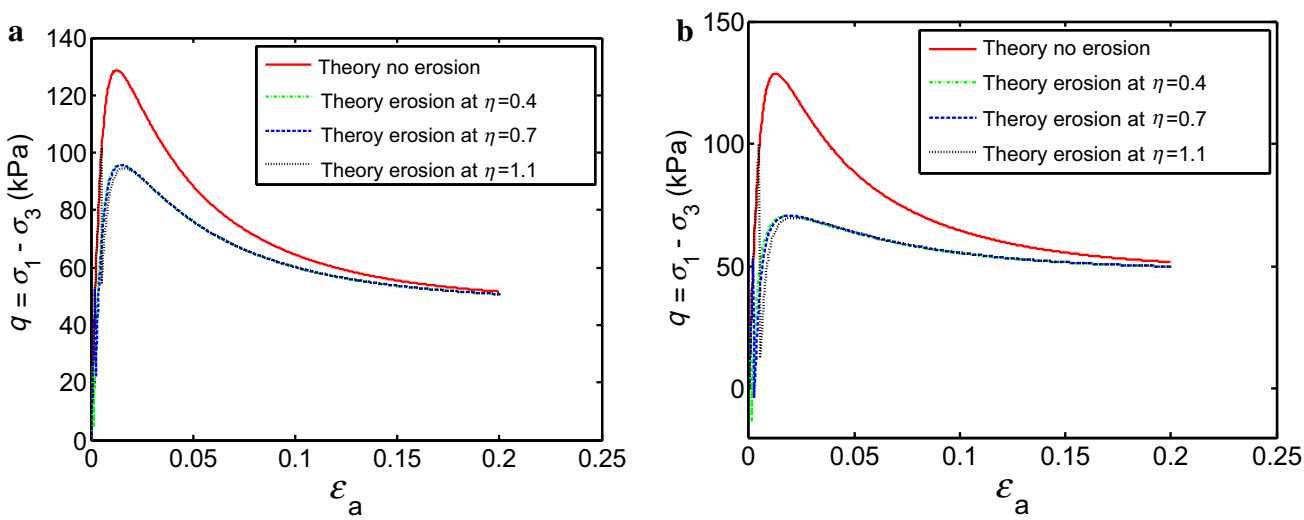

Fig. 14 Constitutive prediction of the mechanical behavior of the granular material under internal erosion in triaxial compression test for different stress states when erosion happens. **a** Cases for 2 % mass erosion. **b** Cases for 4 % mass erosion

trends of the degradation due to internal erosion are consistent with the DEM simulation results, as can be observed in Fig. 13. The peak strength is reduced, and the dilatancy also decreases as a result of internal erosion. Conspicuous mass erosion induces more remarkable degradation. However, the residual friction angle seems to be unchanged no matter how much mass of particles is removed. The fact is proved by either DEM simulation or constitutive relationship prediction. Meanwhile, the experimental result of Chang and Zhang [4] also shows that the peak friction angles drops obviously, but the residual strength only varies little after internal erosion. With regard to the evolution of porosity, a sudden increase due to the 'loose' effect is at first observed, and then after FND and FNR, a volume contraction is found as most of the dense granular materials behave. After that, the volume expands until critical state is approached. However, the prediction for conspicuous mass erosion seems to be a bit lower than the DEM simulation.

5.3 Response prediction for different stress states in internal erosion

The stress state also plays an important role in the internal erosion behavior, in particular in the hydraulic and erosion process. When consolidation finishes, a triaxial loading is firstly applied to the stress ratios ($\eta = \frac{q}{p}$) of 0, 0.4, 0.7, and 1.1, corresponding to different stress states. In each stress state, particle removal is implemented in the DEM simulation with different mass erosion percentages. The prediction by the constitutive law is shown in Fig. 14 for mass

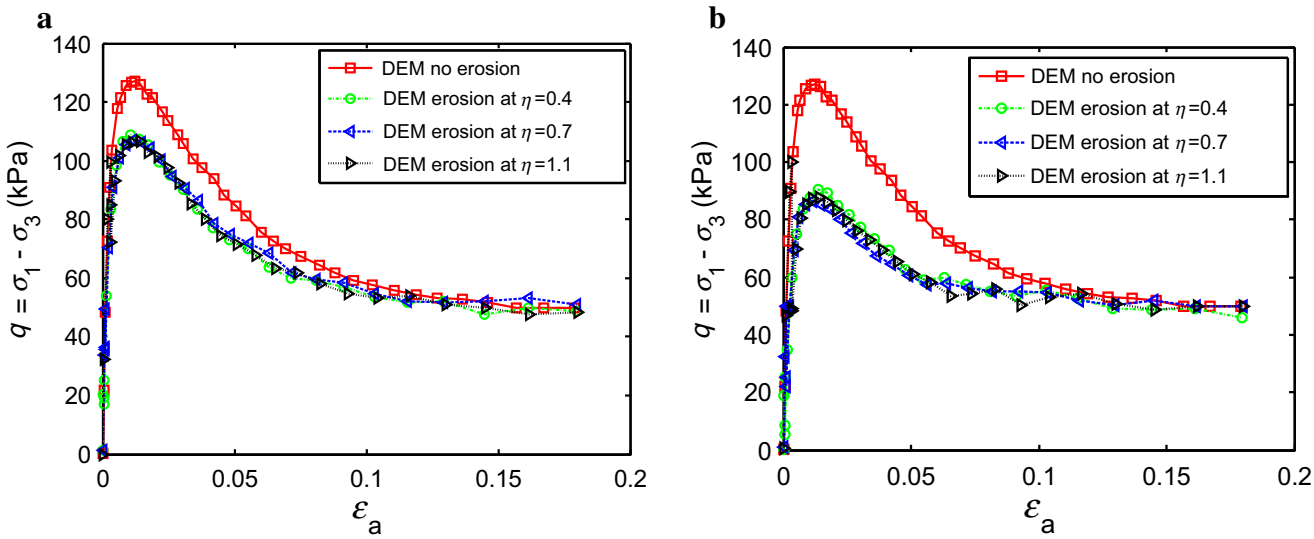

Fig. 15 DEM simulation of the mechanical behavior of the granular material under internal erosion in triaxial compression test for different stress states when erosion happens. **a** Cases for 2 % mass erosion. **b** Cases for 4 % mass erosion

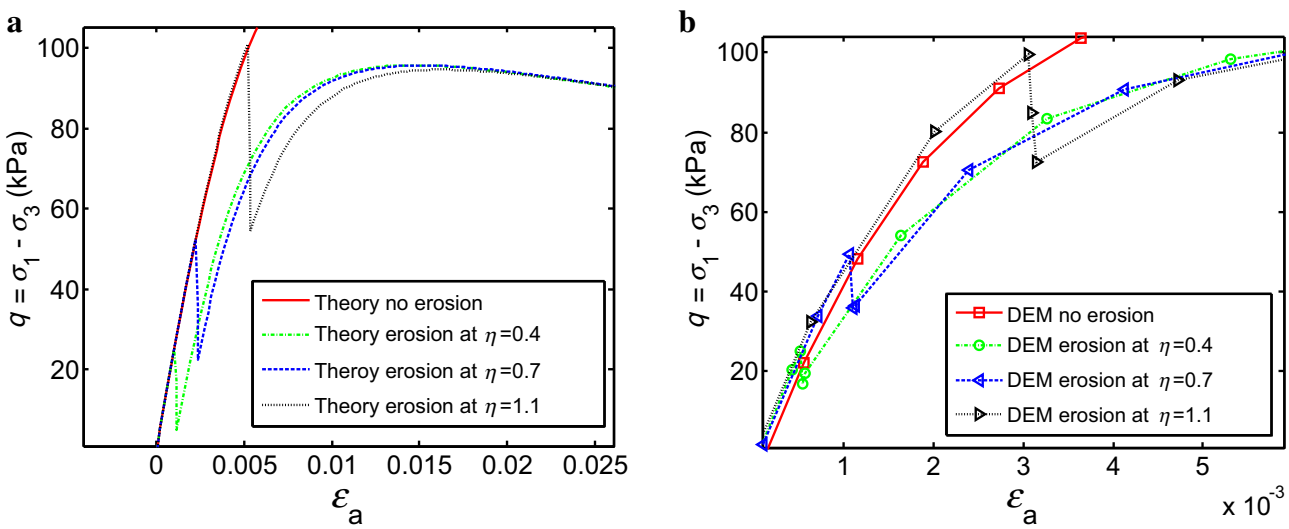

Fig. 16 Sudden stress reduction when particle erosion happens for 2 % mass erosion at different stress states. **a** Constitutive prediction. **b** DEM simulation

erosion of 2 % and 4 %, respectively, at different stress ratios. Figure 15a plots the DEM simulation results. The particle removal strongly degrades the granular materials to a new material. For small mass erosion at small stress ratio, the granular assembly with internal erosion will follow the behavior of the degraded granular material as shown in Figs. 14a and 15a for both constitutive prediction and DEM simulation.

However, for conspicuous mass erosion at high stress ratio, a sudden stress decrease is observed as shown in Figs. 14b and 16b, then the granular assembly will follow the behavior of the strongly degraded granular materials. Actually, the sudden reduction of stress, much like the unloading process in classical uniaxial test or triaxial test for a specimen, does exist in all the erosion cases. This phenomenon can be observed by amplification of the local region near the internal erosion points in Fig. 14 and Fig. 15. Fig. 16 and Fig. 17 provide quantitative results for mass erosion percentages of 2, and 4 %, respectively. The sudden reduction by FND and FNR are clearly observed in Figs. 16 and 17 for either low mass erosion or high mass erosion. However, this kind of phenomenon needs to be validated in realistic experiment.

For the cases of low mass erosion at low stress state, such as 2 % at a stress ratio of 0.4, stress will recover to the original stress state after some loads. Without considering this

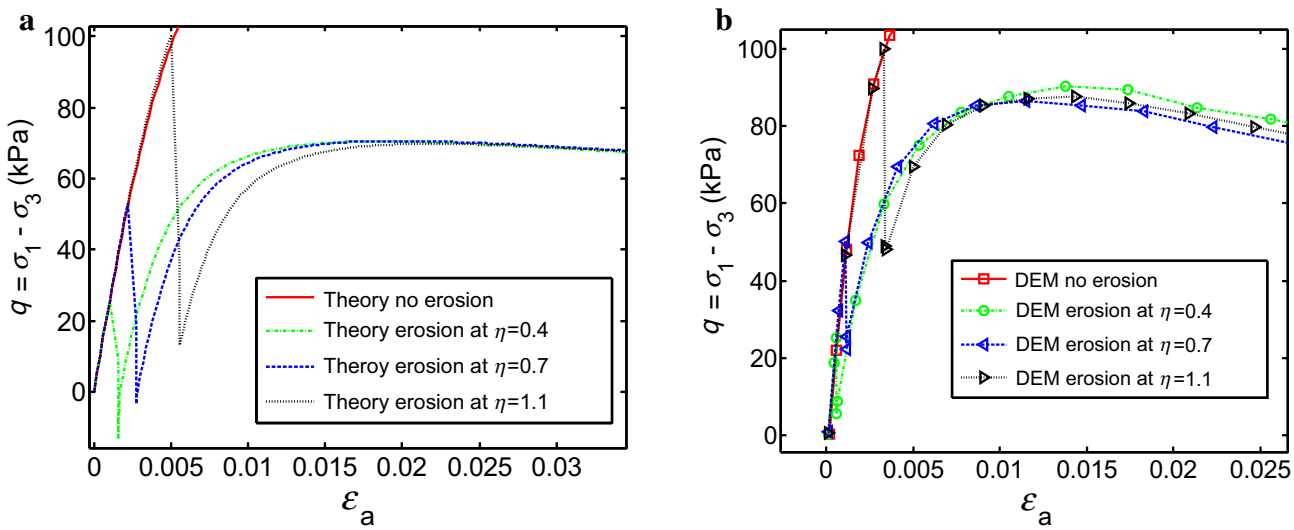

Fig. 17 Sudden stress reduction when particle erosion happens for 4 % mass erosion at different stress states. **a** Constitutive prediction. **b** DEM simulation

short reduction and loading process, one could attribute the effect of internal erosion into a volume reduction without any damage or relaxation in the stress, which is used by Papamichos [10] and Hicher [12]. However, for large mass erosion at high stress states, such as 4 % at stress ratio of 1.1, the force network damage and relaxation are so strong that the stress will no longer recover to its original stress state, which cannot be predicted by the model of either Papamichos [10] or Hicher [12]. Namely, when high mass erosion happens at large stress states, the constitutive law considering FND and FNR is able to predict the mechanical responses since FND and FNR have taken into account the primary mechanism of internal erosion. On the other hand, triaxial loading in triaxial compression is applied just at the moment particles are removed, and the FND and FNR processes start simultaneously in DEM simulation. Hence, it is not strange that the prediction of the sudden stress reduction in DEM simulation is lower than the theoretical prediction.

6 Conclusion

In this study, a state-based elasto-plastic constitutive law accounting for internal erosion along with a discrete element model in triaxial compression is established to simulate the influences of particle removal on mechanical behavior of granular materials. Four essential effects of internal erosion on the degradation of granular materials, including loose effect, force network damage, force network relaxation and variation of critical state, have been incorporated into the constitutive law to form a unified description for the degradation of granular materials due to internal erosion. The agreement between theoretical prediction and DEM simulation such as the reduction of peak strength/dilatancy and, in particular, the sudden stress reduction process during internal erosion demonstrates that this new constitutive formulation is a potential scheme to describe the degradation of granular materials with internal erosion. The volume contraction in the internal erosion only happens when the erosion mass percentage is remarkable. However, this model still needs further validation by credible experiments. Furthermore, theoretical formulation from mesoscopic physical behavior of force chain, such as elasticity and relaxation [31], may be another promising way to understand the impact of particle removal on the degradation of granular matter. Hopefully, the new model can be coupled with the seepage-internal erosion model [6,7,10] or the fluid-particle interaction method [32] to estimate and assess the risk of piping disaster during flood season.

Acknowledgments The authors appreciate the financial support by National Natural Science Foundation of China (Grants 11432015 and 10932012). The authors would like to thank Dr. Fu, Dr. Zhang, and Mr. Peng for helpful discussion on the mechanism of piping and its modeling.

References

1. Richards, K.S., Reddy, K.R.: Critical appraisal of piping phenomena in earth dams. Bull. Eng. Geol. Environ. **66**, 381–402 (2007)
2. Vardoulakis, I.: Fluidisation in artesian flow conditions: Hydromechanically unstable granular media. Geotechnique **54**, 165–177 (2004)
3. Bendahmane, F., Marot, D., Alexis, A.: Experimental parametric study of suffusion and backward erosion. J. Geotech. Geoenviron. Eng. **134**, 57–67 (2008)

4. Chang, D.S., Zhang, L.M.: A stress-controlled erosion apparatus for studying internal erosion in soils. Geotech. Test. J. **34**, 579–589 (2011)
5. Foster, M., Fell, R.: Assessing embankment dam filters that do not satisfy design criteria. J. Geotech. Geoenviron. Eng. **127**, 398–407 (2001)
6. Fujisawa, K., Murakami, A., Nishimura, S.-I.: Computational method to analyze internal erosion and transport of soil particles. Trans. Jpn Soc Irrig. Drain. Rural Eng. **77**, 85–93 (2009)
7. Peng, B., Zhang, Z.: Numerical simulation of seepage failure of levee foundation. In: Proceedings of the 14th Asian Congress of Fluid Mechanics. Hanoi and Halong, Vietnam, 15–19 Oct. (2013)
8. Bonelli, S.: Erosion of Geomaterials. Wiley, London (2012)
9. Fu, Z.D., Li, J.C.: Strength softening models of soil and its application in rainfall-induced landslide simulation. Theor. Appl. Mech. Lett. **3**, 042002 (2013)
10. Papamichos, E.: Erosion and multiphase flow in porous media application to sand production. Eur. J. Environ. Civ. Eng.**14**, 1129–1154 (2010)
11. Papamichos, E., Vardoulakis, I., Tronvoll, J., et al.: Volumetric sand production model and experiment. Int. J. Numer. Anal. Methods Geomech. **25**, 789–808 (2001)
12. Hicher, P.Y.: Modelling the impact of particle removal on granular material behaviour. Geotechnique **63**, 118–128 (2013)
13. Sterpi, D.: Effects of the erosion and transport of fine particles due to seepage flow. Int. J. Geomech. **3**, 111–122 (2003)
14. Fujisawa, K., Murakami, A., Nishimura, S., et al.: Simultaneous modeling of internal erosion and deformation of soil structures. Geoenviron. Eng. Geotech. **204**, 71–78 (2010)
15. Scholtès, L., Hicher, P.-Y., Sibille, L.: Multiscale approaches to describe mechanical responses induced by particle removal in granular materials. C. R. Mec. **338**, 627–638 (2010)
16. Manzari, M.T., Dafalias, Y.F.: A critical state two-surface plasticity model for sands. Geotechnique **47**, 255–272 (1997)
17. Cubrinovski, M.T., Ishihara, K.: Modeling of sand behavior based on state concept. Soils Found. **38**, 115–127 (1998)
18. Gajo, A., Wood, M.: Severn-Trent sand: A kinematic-hardening constitutive model: the q-p formulation. Geotechnique **49**, 595–614 (1999)
19. Houlsby, G.: The work input to an unsaturated granular material. Geotechnique **47**, 193–196 (1997)
20. Wan, R., Guo, P.: A simple constitutive model for granular soils: Modified stress-dilatancy approach. Comput. Geotech. **22**, 109–133 (1998)
21. Li, X., Dafalias, Y.: Dilatancy for cohesionless soils. Geotechnique **50**, 449–460 (2000)
22. Wood, D.M.: Geotechnical Modelling. Taylor & Francis, New York (2003)
23. Been, K., Jefferies, M.: A state parameter for sands. Geotechnique **35**, 99–112 (1985)
24. Gao, Z.W., Zhao, J.D., Li, X.S., et al.: A critical state sand plasticity model accounting for fabric evolution. Int. J. Numer. Anal. Methods Geomech. **38**, 370–390 (2014)
25. Scholtes, L., Hicher, P.Y., Sibille, L.: Multiscale approaches to describe mechanical responses induced by particle removal in granular materials. C. R. Mec. **338**, 627–638 (2010)
26. Wang, X.L., Li, J.C.: Numerical triaxial apparatus and application. Appl. Mech. Mater. **353**, 3251–3255 (2013)
27. Muir Wood, D., Maeda, K.: Changing grading of soil: effect on critical states. Acta. Geotech. **3**, 3–14 (2008)
28. Cundall, P.A., Strack, O.D.L.: A discrete numerical model for granular assemblies. Geotechnique **29**, 47–65 (1979)
29. Kozicki, J., Donze, F.V.: Yade-open dem: an open-source software using a discrete element method to simulate granular material. Eng. Comput. **26**, 786–805 (2009)
30. Wang, X.L., Li, J.C.: Simulation of triaxial response of granular materials by modified DEM. Sci. China-Phys. Mech. Astron. **57**, 2297–2308 (2014)
31. Sun, Q.C., Song, S.X., Jin, F., et al.: Elastic energy and relaxation in triaxial compressions. Granul. Matter. **13**, 743–750 (2011)
32. Zhao, J.D., Shan, T.: Numerical modeling of fluid-particle interaction in granular media. Theor. Appl. Mech. Lett. **3**, 021007 (2013)